Analysis of inclusive (d,xp) reactions on nuclei from ^{9}Be to ^{238}U at 100 MeV

Tao Ye
Institute of Applied Physics and Computational Mathematics, Beijing 100094, China

Shintaro Hashimoto*
Advanced Science Research Center, Japan Atomic Energy Agency, Ibaraki 319-1195, Japan

Yukinobu Watanabe
Department of Advanced Energy Engineering Science, Kyushu University, Fukuoka 816-8580, Japan

Kazuyuki Ogata
Research Center of Nuclear Physics (RCNP), Osaka University, Ibaraki 567-0047, Japan

Masanobu Yahiro
Department of Physics, Kyushu University, Fukuoka 812-8581, Japan
(Received 26 April 2011; published 4 November 2011)

Inclusive proton emissions from deuteron-induced reactions on ^{9}Be, ^{12}C, ^{27}Al, ^{58}Ni, ^{93}Nb, ^{181}Ta, ^{208}Pb, and ^{238}U at an incident energy of 100 MeV are analyzed using the continuum discretized coupled-channels theory for the elastic-breakup process and the Glauber model for the neutron-stripping process in order to investigate deuteron-breakup processes over a wide range of target mass numbers. The effects of Coulomb interactions are taken into account to give a proper description of proton emissions at forward angles. Moreover, the phenomenological moving-source model is used to estimate evaporation and preequilibrium components in inclusive (d,xp) spectra. The calculation reproduces fairly well a prominent bump observed around half the incident energy in experimental (d,xp) spectra for light and medium nuclei at forward angles of less than 20° whereas the calculation underestimates the bump component as the target atomic number increases. The underestimation is likely due to the fact that the eikonal approximation used in the Glauber model becomes worse due to strong Coulomb interactions. It is shown that the Glauber-model calculation for the neutron-stripping process leads to an improvement of this discrepancy by substituting the eikonal phase shift for the quantum phase shift given by the optical-model calculation.

DOI: 10.1103/PhysRevC.84.054606 PACS number(s): 24.10.−i, 25.45.−z, 24.50.+g

I. INTRODUCTION

Recently, research and development of intensive accelerator-driven neutron sources has lead to renewed interest in the study of deuteron-induced reactions. For instance, the Li(d,xn) reaction is regarded as one of the most promising reactions to produce intense neutron beams at the International Fusion Material Irradiation Facility (IFMIF) [1]. Comprehensive nuclear data of deuteron-induced reactions over wide ranges of incident energy and target mass number are indispensable for the accurate estimation of neutron yields and induced radioactivities in the engineering design of accelerator-driven neutron sources. In the cases in which experimental data are not available, theoretical-model calculations play a key role in nuclear-data production.

Nucleon emission from deuteron-induced reactions takes place via various processes: deuteron elastic (or diffractive) breakup and nucleon-stripping processes, sequential particle emission from highly excited compounds and residual nuclei, and so on. Thus, one needs theoretical-model calculations in which all these processes are consistently taken into account. In particular, treatment of both the breakup and stripping processes are of essential importance in predicting neutron yields because the deuteron is a very loosely bound system.

In our early work, we proposed a model calculation method that is capable of describing inclusive nucleon emissions quantitatively and applied it to inclusive nucleon emissions from deuteron-induced reactions on ^{7}Li and ^{12}C up to 100 MeV [2,3]. The model calculations use the continuum discretized coupled-channels (CDCC) method [4–6] for the elastic-breakup process, the Glauber model [7] for the nucleon-stripping process, and the moving-source model [8] for the preequilibrium and evaporation processes. The results showed quite good agreement between the calculations and recent experimental data.

As the next step, it is interesting to investigate the applicability of our proposed calculation method to inclusive nucleon emission from deuteron-induced reactions over a wide target-mass-number range. Although neutron-emission data are necessary given our motivation of engineering applications, there are no available experimental data of double-differential (d,xn) cross sections in the incident-energy range of interest

*Nuclear Science and Engineering Directorate, Japan Atomic Energy Agency, 2-4 Shirane, Shirakata, Tokai-mura, Naka-gun, Ibaraki 319-1195, Japan.

except for the Li(d,xn) reaction at 40 MeV [9], which we analyzed in our early work [2,3]. On the other hand, thick-target neutron-yield (TTNY) data do exist [10]. In this case, neutrons are emitted from deuteron-induced reactions at energies ranging from the incident energy down to zero energy because of energy loss in the thick target. The transport of the incident deuteron in the thick target should be taken into account properly for comparison with the measurements. Thus, TTNY data are not appropriate for the validation of the nuclear-reaction model itself. In the present work, therefore, we have analyzed the double-differential cross sections of inclusive (d,xp) reactions, which were measured systematically for ^{9}Be, ^{12}C, ^{27}Al, ^{58}Ni, ^{93}Nb, ^{181}Ta, ^{208}Pb, and ^{238}U at an incident energy of 100 MeV by Ridikas *et al.* [11]. In our previous calculations, the dissociation of the deuteron via Coulomb interactions with the target nucleus was neglected because the atomic numbers of both target nuclei, i.e., ^{7}Li and ^{12}C, are small. However, it is expected that the Coulomb dissociation would play an essential role in the collision between a loosely bound projectile and a heavy target nucleus [12–14]. Thus, we explicitly take into account the Coulomb dissociation in CDCC calculations and investigate its effect on inclusive (d,xp) reactions.

In Sec. II, we briefly describe the model calculations and the treatment of the Coulomb breakup. The effect of the Coulomb breakup and calculation results of the (d,xp) reactions on various targets at 100 MeV are presented and discussed in Sec. III. Finally, our conclusions are given in Sec. IV.

II. THEORETICAL MODEL

Various reaction processes are involved in inclusive nucleon emissions from deuteron-induced reactions: the direct processes, i.e., the elastic-breakup and stripping processes, and the statistical decay processes, i.e., the preequilibrium and evaporation processes. We use the same model approach as proposed in Ref. [2] to analyze the experimental (d,xp) data. For the direct processes, the CDCC method is applied to the calculations of the elastic-breakup (EB) process, and the Glauber model is used for those of the nucleon-stripping process (STR) in the continuum. Moreover, we use the moving-source (MS) model [8] to estimate the evaporation and preequilibrium components (EP). Finally, the double-differential cross sections (DDXs) of (d,xp) reactions are expressed by the incoherent summations of these three components:

$$\frac{d^2\sigma^{(d,xp)}}{dE_p^L d\Omega_p^L} = \left.\frac{d^2\sigma_{\rm EB}}{dE_p^L d\Omega_p^L}\right|_{\rm CDCC} + \left.\frac{d^2\sigma^n_{\rm STR}}{dE_p^L d\Omega_p^L}\right|_{\rm Glauber} + \left.\frac{d^2\sigma_{\rm EP}}{dE_p^L d\Omega_p^L}\right|_{\rm MS}, \quad (1)$$

where the superscript L stands for physical quantities in the laboratory system. Details of each model are given in Ref. [2].

In the CDCC method, the Coulomb breakup of the deuteron can be treated by accounting for the Coulomb interaction between the proton and the target exactly, replacing $V_{\rm Coul}(\vec{R}_{d\rm A})$ with $V_{\rm Coul}(\vec{r}_{p\rm A})$, where $\vec{R}_{d\rm A}$ represents the displacement between the center of mass of the deuteron and that of the target and $\vec{r}_{p\rm A}$ denotes the displacement between the proton in the deuteron and the center of mass of the target. In the case of a light target nucleus, the effect of the Coulomb breakup is small, and the experimental data can be well described using $V_{\rm Coul}(\vec{R}_{d\rm A})$ [2–6].

The differential cross section for the neutron-stripping process is given in the center of mass of the p-n system by the following expression based on the Glauber model [15]:

$$\frac{d\sigma^n_{\rm STR}}{d\vec{k}_p^C} = \frac{1}{(2\pi)^3}\int d^2\vec{b}_n \left\{[1-|S_n(b_n)|^2] \times \left|\int d^3\vec{r}\; e^{-i\vec{k}_p^C\cdot\vec{r}} S_p(b_p)\psi_{00}(\vec{r})\right|^2\right\}, \quad (2)$$

where b_p and b_n are the impact parameters of the proton and neutron perpendicular to the z axis, $\vec{r}$ is the relative coordinate between the proton and neutron in the deuteron, $\vec{k}_p^C$ is the proton-wave-number vector, and $\psi_{00}(\vec{r})$ is the wave function of the deuteron ground state. The Coulomb interaction is included in the S matrix to describe the interaction between the proton and the target, which is defined by

$$S_p(b_p) = e^{i\chi_{p\rm A}(b_p)} = \exp\left[-\frac{i}{\hbar\upsilon}\int_{-\infty}^{+\infty} dz\; V_{p\rm A}\left(\sqrt{b_p^2+z^2}\right)\right], \quad (3)$$

where $V_{p\rm A}$ includes both the nuclear and Coulomb interactions between the proton and the target. Since the integral in Eq. (3) for the Coulomb interaction diverges, we use the same prescription as in Ref. [16] in which $\chi_{p\rm A}(b_p) = \chi^{\rm N}_{p\rm A}(b_p) + \chi^{\rm C}_{p\rm A}(b_p)$, where $\chi^{\rm N}_{p\rm A}(b_p)$ is calculated using a phenomenological optical potential without the Coulomb potential and the Coulomb eikonal phase shift is chosen as $\chi^{\rm C}_{p\rm A}(b_p)$ in the same way as in Refs. [2,3].

The moving-source model is a phenomenological method of estimating nucleon emissions via statistical decay processes. Using the same procedure as described in Refs. [2,3], the parameters involved in it are determined by fitting the experimental DDXs at backward angles at which the direct breakup and stripping components are negligibly small.

III. RESULTS AND DISCUSSION

Inclusive (d,xp) reactions on eight targets from ^{9}Be to ^{238}U at 100 MeV are analyzed using the models outlined in Sec. II. The CDCC calculations are performed using the same codes as those in Refs. [13,17]. The major input data necessary in the Glauber-model calculation are the nucleon optical-model potential (OMP) and the deuteron-ground-state wave function, which are the same as those in the CDCC calculation. Both the CDCC and Glauber-model calculations use the Watson OMP for ^{9}Be and ^{12}C [18] and the nucleon OMP given by Koning and Delaroche [19] for other heavier targets at half the incident deuteron energy.

First, we investigate the effects of the Coulomb elastic breakup in deuteron-induced reactions. The Coulomb interaction between the deuteron and the target nucleus becomes stronger as the target atomic number Z increases. Therefore, the incident deuteron is expected to dissociate easily into a

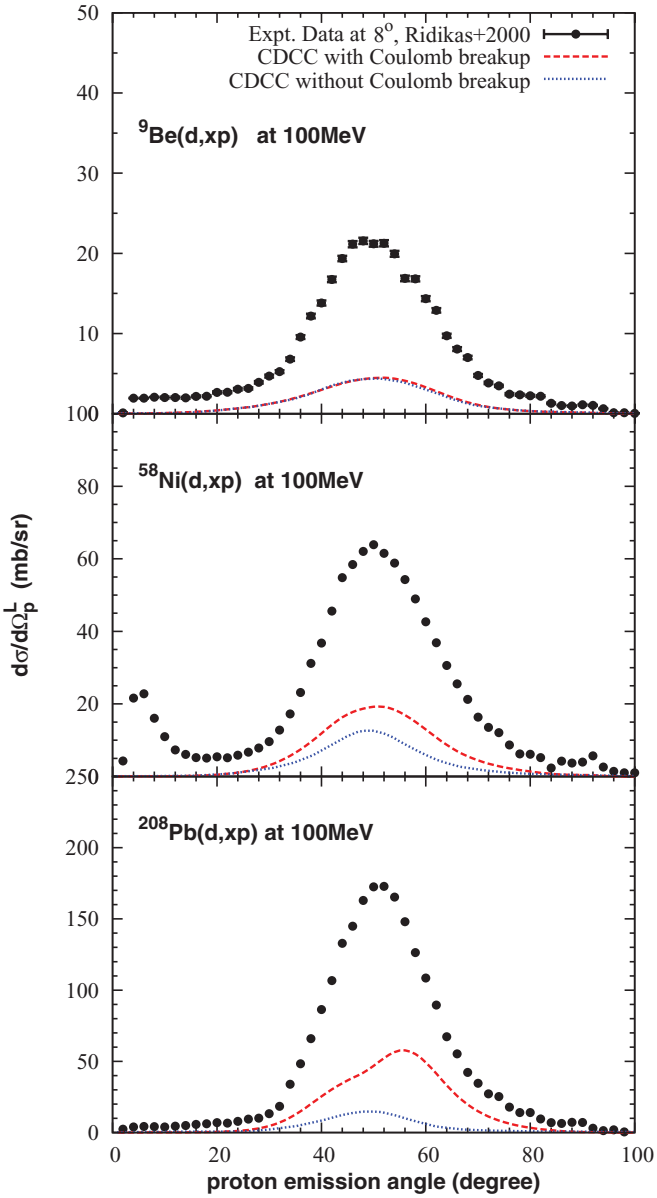

FIG. 1. (Color online) Comparison of CDCC calculations with and without Coulomb breakup in (d,xp) reactions on ^{9}Be, ^{58}Ni, and ^{208}Pb at 100 MeV and 8°. The experimental data are from Ref. [11].

neutron and a proton in the case of high-Z target nuclei. Figure 1 shows comparisons of the calculated DDXs of 100-MeV (d,xp) reactions using the CDCC method with and without the Coulomb-breakup process on three targets, ^{9}Be, ^{58}Ni, and ^{208}Pb, at 8°. It is obvious that the effect of the Coulomb elastic breakup becomes prominent with an increase of the target atomic number. Moreover, the calculations considerably underestimate the measurements over the entire emission-energy range. This indicates that the other reaction processes must be involved in proton emission, i.e., neutron stripping to the continuum, preequilibrium, and evaporation processes.

Next, the DDXs calculated with Eq. (1) are shown for ^{9}Be, ^{27}Al, ^{58}Ni, ^{93}Nb, and ^{208}Pb at forward emission angles along with experimental values [11] in Figs. 2–6. Comparisons

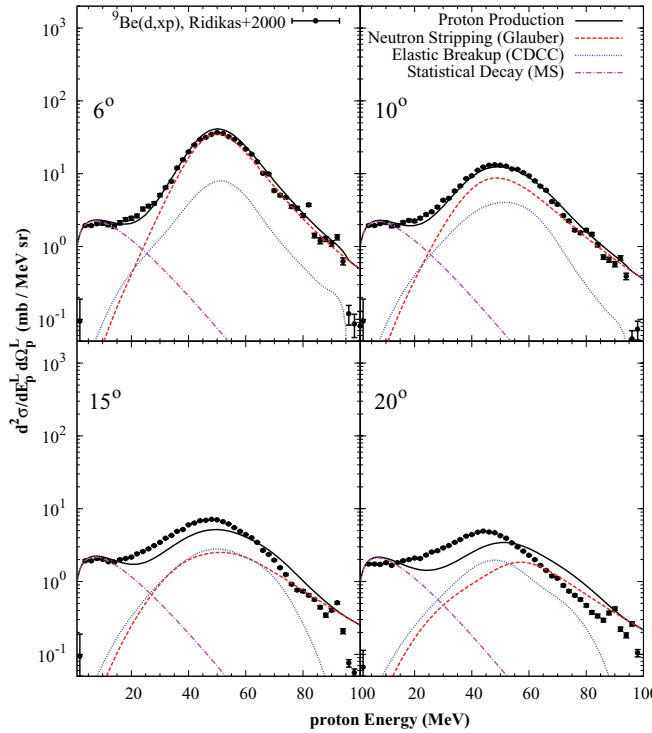

FIG. 2. (Color online) Comparison of the calculated DDXs of ^{9}Be(d,xp) at 100 MeV with the experimental data for different proton emission angles. The experimental data (dots) are from Ref. [11].

between the calculated and experimental DDXs at 8° are made for all the targets to determine the manner in which they vary with the target atomic number in Fig. 7. In these

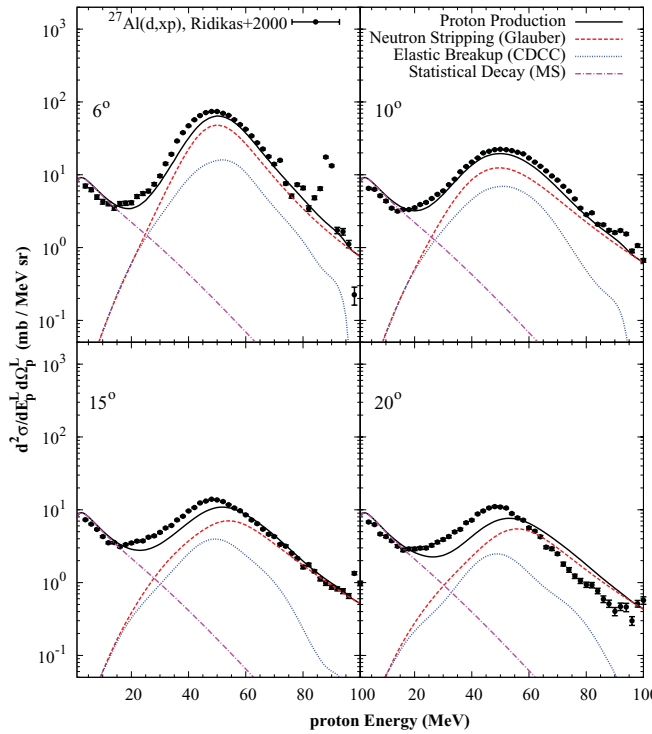

FIG. 3. (Color online) Comparison as in Fig. 2 for the target nucleus ^{27}Al.

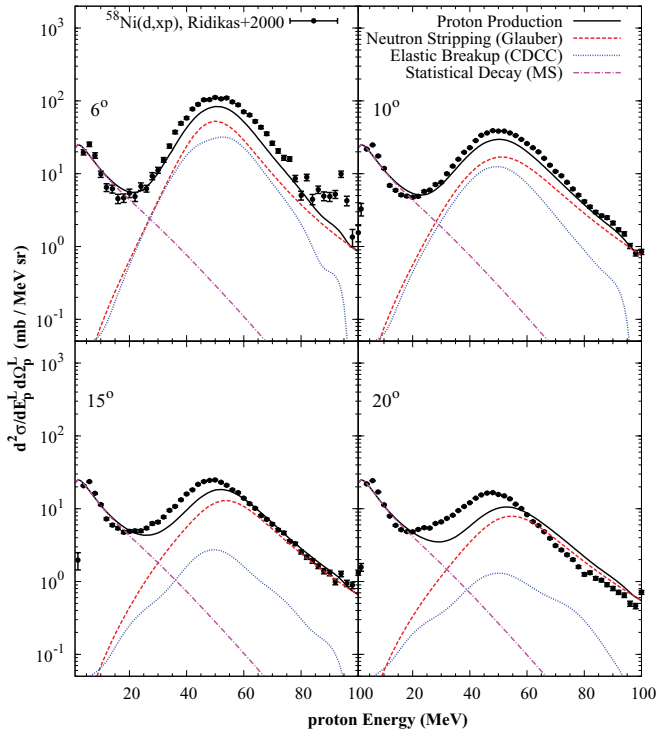

FIG. 4. (Color online) Comparison as in Fig. 2 for the target nucleus ^{58}Ni.

figures, the dotted curves correspond to the elastic-breakup components calculated with the CDCC method, and the dashed curves represent the neutron-stripping components calculated

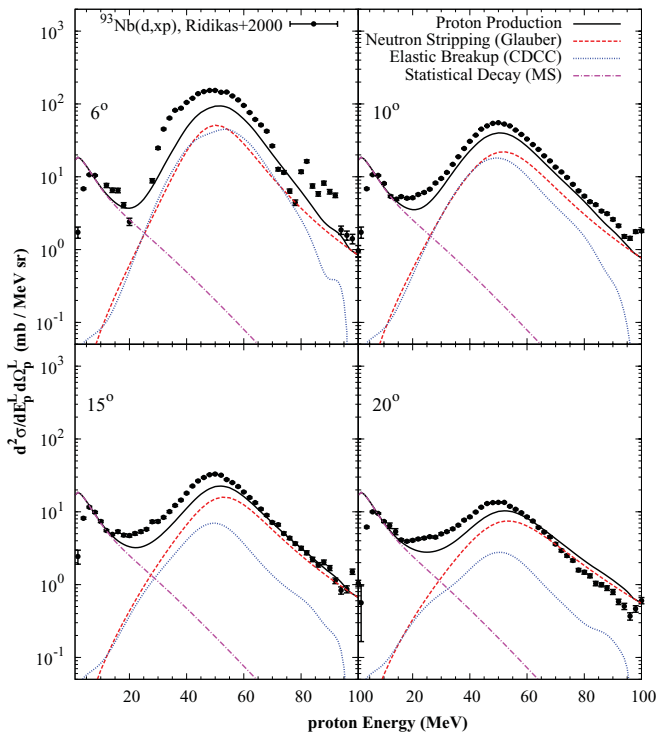

FIG. 5. (Color online) Comparison as in Fig. 2 for the target nucleus ^{93}Nb.

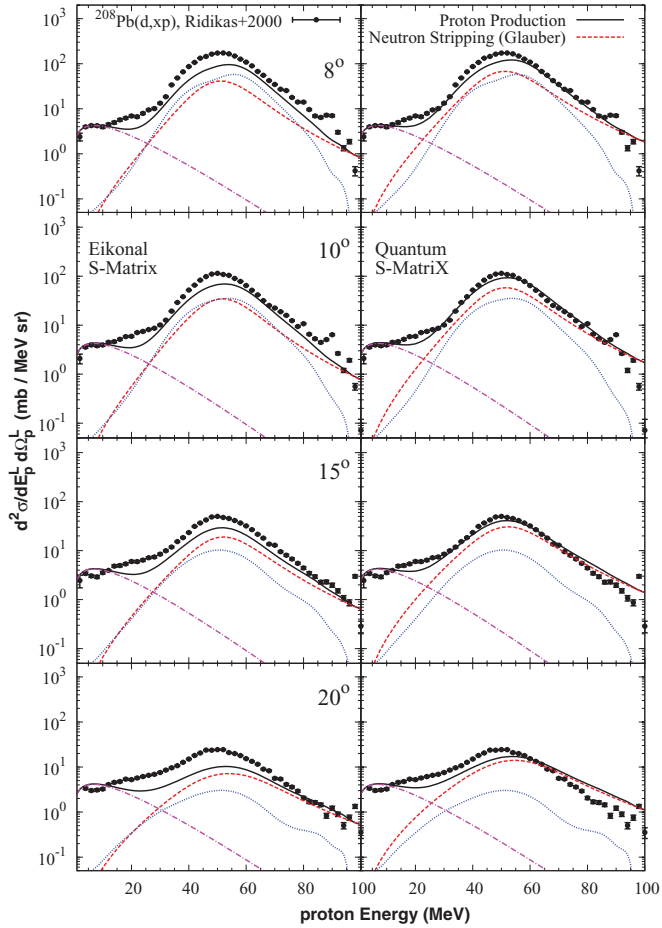

FIG. 6. (Color online) Comparison as in Fig. 2 for the target nucleus ^{208}Pb. The Glauber-model calculation with the same eikonal phase shift as in Figs. 2–5 is shown on the left and that with the quantum phase shift on the right.

with the Glauber model. The evaporation and preequilibrium components plotted by the dot-dashed curves are estimated using MS-model calculations. The parameters used in the MS model were determined by fitting the experimental data at backward angles at which the contribution from direct processes is expected to be negligibly small. As an example, Fig. 8 shows the case of ^{58}Ni for proton emission at 120°. The parameters obtained for all the targets are summarized in Table I. As can be seen from Figs. 2–7, the calculations are in good agreement with the measurements for the target nuclei up to ^{58}Ni in both shape and magnitude except at 20°. Meanwhile, the calculations for heavier target nuclei, i.e., ^{208}Pb (see the left side of Fig. 6), underestimate the experimental data by a factor of about 2 around the center of the broad peak. In addition, Fig. 7 reveals an interesting trend in which the relative fraction of the elastic-breakup process increases with the target atomic number whereas the neutron-stripping component calculated with the Glauber model increases gradually with the target atomic number, and the Coulomb effect is less appreciable than that seen in the CDCC calculations for the elastic-breakup process.

Here, we examine the effect of the Coulomb interactions on the Glauber-model calculations and consider the

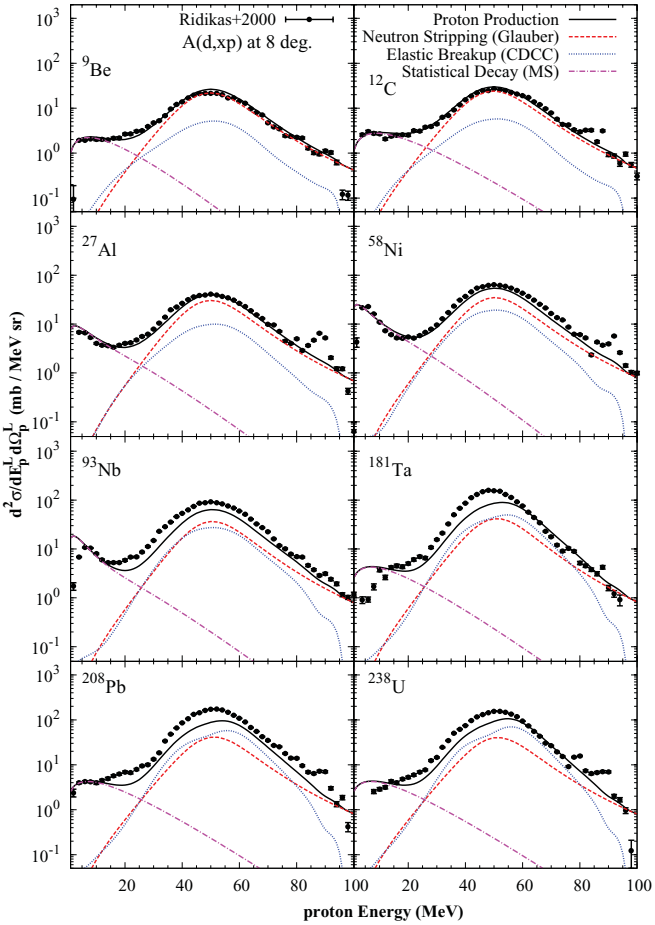

FIG. 7. (Color online) Comparison of the calculated DDXs of (d,xp) reactions at 100 MeV with the experimental data for 8° on different targets from ^{9}Be to ^{238}U. The experimental data (dots) are from Ref. [11].

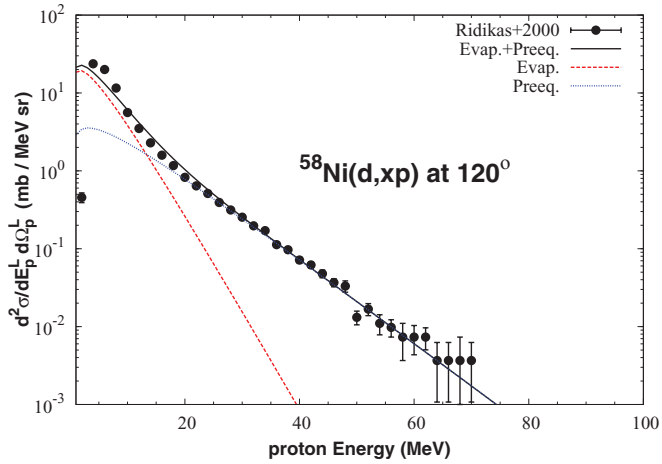

FIG. 8. (Color online) Fitting of the experimental data of ^{58}Ni(d, xp) at 100 MeV and 120° using the moving-source model. The dotted and dashed curves represent the components of the evaporation and preequilibrium processes, respectively. The solid curve gives their sum.

underestimation seen in the (d,xp) spectra for high-atomic-number nuclei. Brooke *et al.* [20] proposed a noneikonal calculation for the scattering of loosely bound n-cluster composite nuclei by replacing the eikonal phase shift with the quantum partial-wave phase shift to noninteger angular momenta and demonstrated that this method is more accurate for energies as low as 10 MeV/nucleon than the eikonal approximation. We have decided to incorporate a similar noneikonal approach into our Glauber-model calculations of the neutron-stripping process to see noneikonal effects on the inclusive neutron-stripping process. The eikonal S matrices used in the Glauber-model calculations are replaced by the quantum S matrices given by the optical-model calculations with the ECIS code [21]. For simplicity, we transform the quantum S matrix given for the integer orbital angular momentum L into that for the corresponding impact parameter b using the relation $kb = \sqrt{L(L+1)}$, where k is the wave number.

Figure 9 shows comparisons of the moduli of the S matrices for the neutron and proton for ^{208}Pb at incident energies of 50, 100, and 200 MeV as functions of L. Both S matrices coincide with each other as the incident energy increases, confirming the effectiveness of the eikonal approximation used in the Glauber model at high energies. The DDXs of the ^{208}Pb(d,xp) reaction at 100 MeV are calculated using the quantum S matrices for 50 MeV at half the incident energy. As shown in Fig. 6, the DDXs calculated with the quantum S matrices [see Fig. 6 (right)] are closer to the experimental data than those with the eikonal S matrices [see Fig. 6 (left)] although some

TABLE I. Parameters of the moving-source model with the following expression: $\frac{d^2\sigma_{\rm EP}}{dE_p^L d\Omega_p^L}|_{\rm MS} = \sum_{i=1,2} N_{0,i}\sqrt{E_p^L}\exp[-(E_p^L + E_{1,i} - 2\sqrt{E_p^L E_{1,i}}\cos\theta_p^L)/T_i]$, where the subscripts $i = 1$ and 2 represent the evaporation and preequilibrium processes, respectively.

Target	$N_{0,1}$ (mb/MeV$^{3/2}$ sr)	$E_{1,1}$ (MeV)	T_1 (MeV)	$N_{0,2}$ (mb/MeV$^{3/2}$ sr)	$E_{1,2}$ (MeV)	T_2 (MeV)
^{9}Be				1.06	2.0	6.98
^{12}C				1.18	2.58	8.30
^{27}Al	8.03	0.0	3.60	1.86	1.2	8.30
^{58}Ni	25.0	0.0	3.30	4.20	1.0	8.00
^{93}Nb	20.0	0.0	3.30	2.20	1.0	8.50
^{181}Ta	1.00	0.0	1.0	2.20	1.0	8.80
^{208}Pb	1.00	0.0	1.0	2.20	1.0	8.80
^{238}U	1.00	0.0	1.0	2.20	1.0	8.80

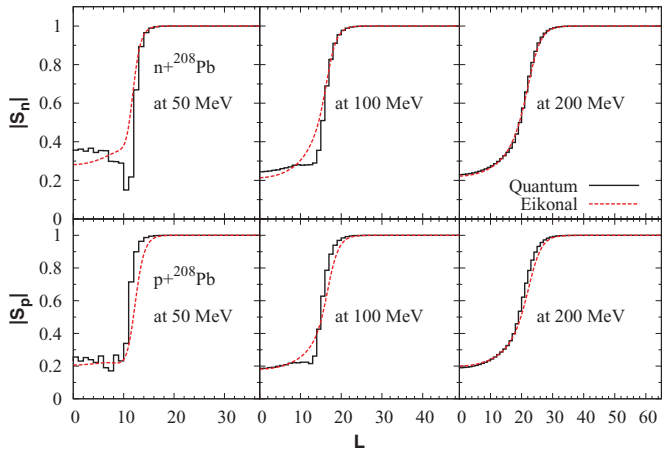

FIG. 9. (Color online) Comparison of the moduli of S matrices of n (or p) incidence on ^{208}Pb given by quantum (solid) and eikonal (dashed) methods, respectively, as a function of angular momentum L at incident energies of 50, 100, and 200 MeV.

underestimation is still seen. The stripping process is known to take place mainly around the peripheral region. The orbital angular momentum corresponding to the impact parameter equal to the radius of ^{208}Pb is about $L = 12$. As shown in Fig. 9, the modulus of the quantum S matrix for the neutron is smaller than that of the eikonal S matrix, and the situation is opposite for the proton. According to the Glauber-model expression given by Eq. (2), the neutron absorption represented by $1 - |S_n(b_n)|^2$ is enhanced, and proton emission becomes preferable in the Glauber-model calculation with the quantum S matrix than with the eikonal S matrix. Thus, we can state that the DDXs calculated using the quantum S matrices are larger than those using the eikonal S matrices.

In Fig. 10, we compare our model calculations for energy-integrated angular distributions of 100-MeV deuteron incidence on ^{9}Be and ^{208}Pb with the experimental data [11]. It is shown that the elastic-breakup and neutron-stripping processes are dominant in proton production at angles less than 30°, and the statistical decay processes provide a major contribution at larger angles. In the case of ^{9}Be, the neutron-stripping process is more predominant than that of the elastic breakup at very small angles whereas in the case of ^{208}Pb, the latter has a larger contribution than the former because the Coulomb breakup easily takes place due to a strong Coulomb interaction. The lower part of Fig. 10 shows that the relative fraction of the neutron-stripping process is enhanced by the Glauber-model calculation with the quantum S matrix, resulting in much better agreement with the experimental data at forward angles.

Ridikas *et al.* [11] have discussed the effect of the Coulomb dissociation of the deuteron in the analysis of their experimental 100-MeV (d,xp) data. The angular distributions calculated using the adiabatic model [14,22,23] are shown for ^{9}Be and ^{208}Pb in Fig. 11 of Ref. [11]. There are some differences between our CDCC calculations and their adiabatic-model calculations. For the lighter nucleus ^{9}Be, the adiabatic-model calculation gives a much smaller differential cross section than the CDCC calculation by a factor of about 6 at 0°.

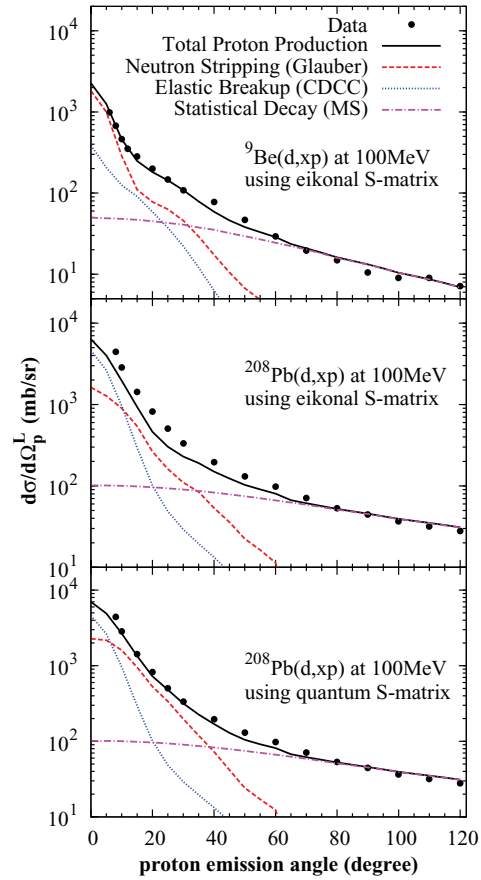

FIG. 10. (Color online) Comparison of the calculated energy-integrated proton angular distributions with the experimental data for 100-MeV deuteron incidence on ^{9}Be and ^{208}Pb. The Glauber-model calculations for ^{208}Pb with the eikonal S matrices (middle) and the quantum S matrices (bottom) are shown for comparison. The experimental data (dots) are from Ref. [11].

The difference can be easily explained by the fact that the CDCC calculation shown in Fig. 10 includes the effect of the nuclear dissociation, which is more predominant compared with the Coulomb dissociation for ^{9}Be as shown in Fig. 1. In contrast, the comparison for ^{208}Pb demonstrates that both calculations provide similar cross sections at very forward angles less than 10°; however, the differential cross sections from the CDCC calculations decrease more rapidly than those from the adiabatic-model calculations at larger emission angles. The adiabatic model of Refs. [14,22,23] switches off the neutron-target interaction (optical potential). This makes absorption of the incident flux significantly weak. When the proton in the deuteron is emitted at relatively large angles, both the proton and neutron pass inside the target nucleus. Thus, the weak absorption is expected to contribute to larger Coulomb-breakup cross sections compared with the present CDCC calculation at large emission angles. It should be noted that the adiabatic model will work well in the cases in which both the proton and neutron are emitted at very forward angles as shown in Ref. [23].

Finally, the variations of the total-proton-production cross sections with target atomic number Z are analyzed in Fig. 11.

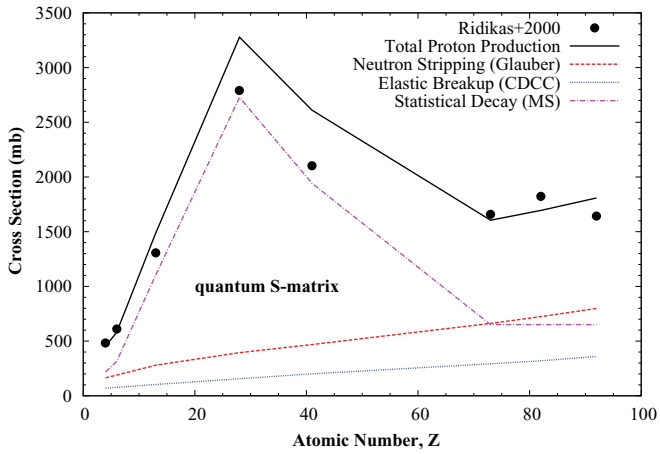

FIG. 11. (Color online) Total-proton-production cross sections as a function of the atomic number Z. The elastic-breakup component calculated by CDCC, the neutron-stripping component calculated by the Glauber model with the quantum S matrix, and the evaporation plus preequilibrium component estimated by the moving-source model are given by the dotted, dashed, and dot-dashed lines, respectively. Their sum is given by the solid line. The experimental data (dots) are from Ref. [11].

Two direct components, i.e., the elastic-breakup and neutron-stripping components, increase monotonically with increasing atomic number and significantly contribute to the proton production for target nuclei with low Z and high Z. Meanwhile, evaporation and preequilibrium components are relatively important in the total (d,xp) cross sections for target nuclei with medium atomic numbers, i.e., ^{27}Al, ^{58}Ni, and ^{93}Nb. Reduction of these components with increasing atomic number is seen for target nuclei heavier than ^{58}Ni. This seems to be explained by the Coulomb barrier effect because the evaporation and preequilibrium components are predominant in the low-proton-energy range as shown in Figs. 2–6.

In the present analysis, the phenomenological moving-source model was used to estimate the evaporation and preequilibrium components. To make the estimation more reliable and predictable for future nuclear-data production, it will be necessary to calculate these statistical decay components with both preequilibrium and Hauser-Feshbach models. In the case of deuteron-induced reactions, the statistical decay calculations become complicated because three different compound nuclei are formed by absorption of either a neutron or a proton or both in the deuteron. However, there is no currently available, general-purpose model code capable of accounting for these compound nuclei properly. Thus, we aim to develop such a code dedicated to deuteron-induced reactions by incorporating the results of the CDCC and Glauber-model calculations into statistical decay calculations as our next step.

IV. SUMMARY AND CONCLUSIONS

Inclusive (d,xp) reactions on ^{9}Be, ^{12}C, ^{27}Al, ^{58}Ni, ^{93}Nb, ^{181}Ta, ^{208}Pb, and ^{238}U at 100 MeV were analyzed systematically using the continuum discretized coupled-channels theory for the elastic-breakup process, the Glauber model for the neutron-stripping process, and the moving-source model for the preequilibrium and evaporation processes. In our analysis, particular attention was paid to the deuteron-breakup processes over the wide atomic-number range of target nuclei. The Coulomb interaction was taken into account in both the calculations of the elastic-breakup and stripping processes.

The calculations reproduced both the shapes and magnitudes of the experimental (d,xp) spectra at forward angles of less than 20° quantitatively well for target nuclei with atomic numbers less than that of ^{58}Ni whereas they underestimated the prominent bump observed around half the incident energy as the target atomic number increased. The analysis revealed that the stripping process is more dominant than the elastic-breakup process for light and medium target nuclei and that the elastic-breakup process is considerably enhanced due to the effect of the Coulomb breakup for heavy target nuclei. It was found that the underestimation seen in the inclusive (d,xp) spectra for high-atomic-number nuclei is improved by replacement of the eikonal S matrix with the quantum S matrix in the Glauber-model expression. This suggests the importance of the noneikonal effect in (d,xp) reactions with high-atomic-number nuclei even at an incident deuteron energy of 100 MeV. Thus, more quantum mechanical approaches beyond the semiclassical Glauber model will be necessary to describe accurately inclusive (d,xp) reactions for high-atomic-number nuclei at relatively low incident energies below 100 MeV.

ACKNOWLEDGMENTS

We would like to thank M. Kawai, Y. Iseri, S. Chiba, and W. Sun for helpful discussions and comments on our analysis. This work was supported by Grants-in-Aid for Scientific Research from the Japan Society for the Promotion of Science (No. 19560844 and No. 22560820). T.Y. is grateful to Project No. 2009B0103009 supported by CAEP, China, for partial support of this work.

[1] H. Matsui, in *Proceedings of the 23rd Symposium on Fusion Technology*, Venice, Italy (2004), pp. 20–24.
[2] T. Ye, Y. Watanabe, and K. Ogata, Phys. Rev. C **80**, 014604 (2009).
[3] Y. Watanabe, T. Ye, and K. Ogata, EPJ Web Conf. **2**, 11003 (2010).
[4] M. Yahiro, Y. Iseri, H. Kameyama, M. Kamimura, and M. Kawai, Prog. Theor. Phys. Suppl. **89**, 32 (1986).
[5] Y. Iseri, M. Yahiro, and M. Kamimura, Prog. Theor. Phys. Suppl. **89**, 84 (1986).
[6] N. Austern, Y. Iseri, M. Kamimura, M. Kawai, G. Rawitscher, and M. Yahiro, Phys. Rep. **154**, 125 (1987).
[7] R. J. Glauber, in *Lectures in Theoretical Physics* (Interscience, New York, 1959), Vol. 1, p. 315.
[8] T. C. Awes, G. Poggi, S. Saini, C. K. Gelbke, R. Legrain, and G. D. Westfall, Phys. Lett. B **103**, 417 (1981).

[9] M. Hagiwara, T. Itoga, N. Kawata, N. Hirabayashi, T. Oishi, T. Yamauchi, M. Baba, M. Sugimoto, and T. Muroga, Fusion Sci. Technol. **48**, 1320 (2005).
[10] M. Hagiwara, T. Itoga, M. Baba, M. S. Uddin, N. Hirabayashi, T. Oishi, and T. Yamauchi, J. Nucl. Mater. **329–333**, 218 (2005).
[11] D. Ridikas, W. Mittig, H. Savajols, P. Roussel-Chomaz, S. V. Förtsch, J. J. Lawrie, and G. F. Steyn, Phys. Rev. C **63**, 014610 (2000); Experimental Nuclear Reaction Data (EXFOR) database file entry: EXFOR-D0489.
[12] F. M. Nunes and I. J. Thompson, Phys. Rev. C **59**, 2652 (1999).
[13] K. Ogata, M. Yahiro, Y. Iseri, T. Matsumoto, N. Yamashita, T. Kamizato, and M. Kamimura, Nucl. Phys. A **738**, 421 (2004).
[14] D. Ridikas, W. Mittig, and J. A. Tostevin, Phys. Rev. C **59**, 1555 (1999).
[15] K. Hencken, G. Bertsch, and H. Esbensen, Phys. Rev. C **54**, 3043 (1996).
[16] C. A. Bertulani and P. G. Hansen, Phys. Rev. C **70**, 034609 (2004).
[17] K. Ogata, S. Hashimoto, Y. Iseri, M. Kamimura, and M. Yahiro, Phys. Rev. C **73**, 024605 (2006).
[18] B. A. Watson, P. P. Singh, and R. E. Segel, Phys. Rev. **182**, 977 (1969).
[19] A. J. Koning and J. P. Delaroche, Nucl. Phys. A **713**, 231 (2003).
[20] J. M. Brooke, J. S. Al-Khalili, and J. A. Tostevin, Phys. Rev. C **59**, 1560 (1999).
[21] J. Rayanl, in *Proceedings of the Specialists' Meeting on the Nucleon Nucleus Optical Model up to 200 MeV*, 13-15 November 1996, Bruyéres-le-Chatel, France, Publication 19 Nuclear Energy Agency, 1997, pp.159-166.
[22] J. A. Tostevin *et al*., Phys. Lett. B **424**, 219 (1998).
[23] J. A. Tostevin, S. Rugmai, and R. C. Johnson, Phys. Rev. C **57**, 3225 (1998).